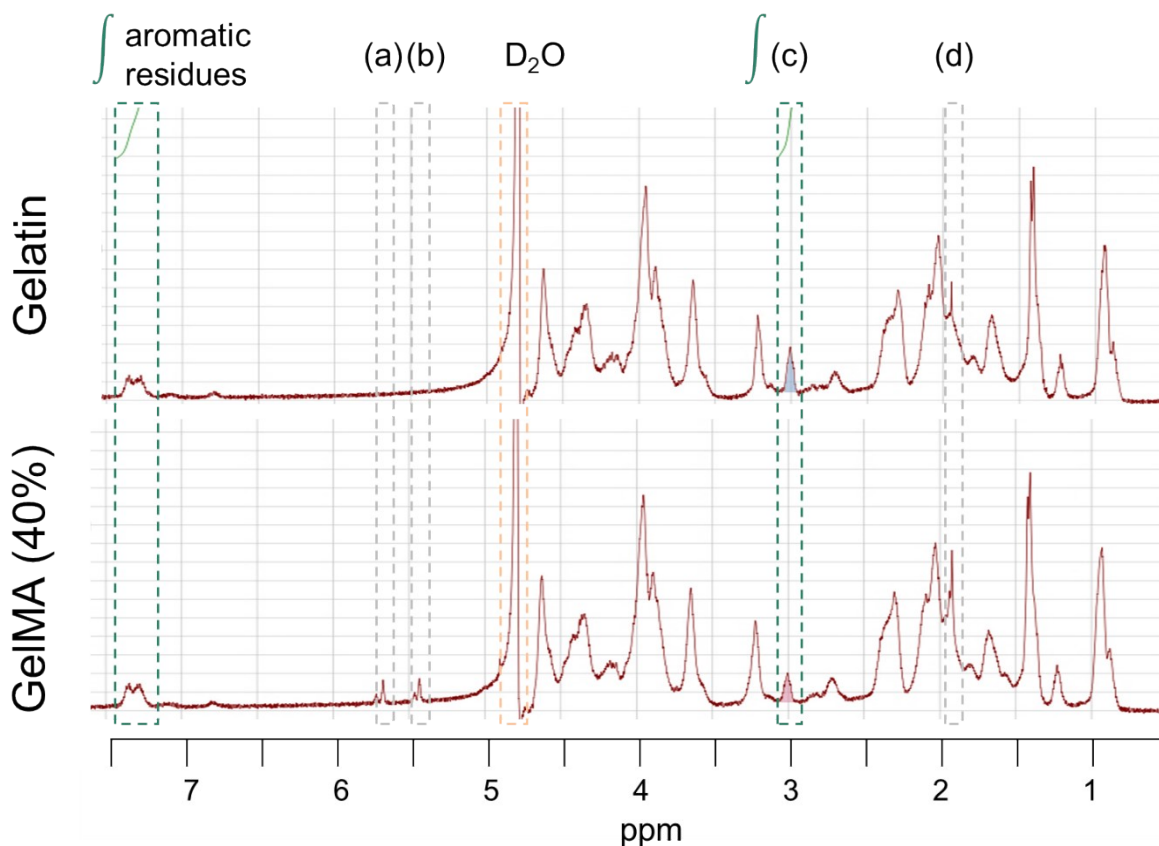
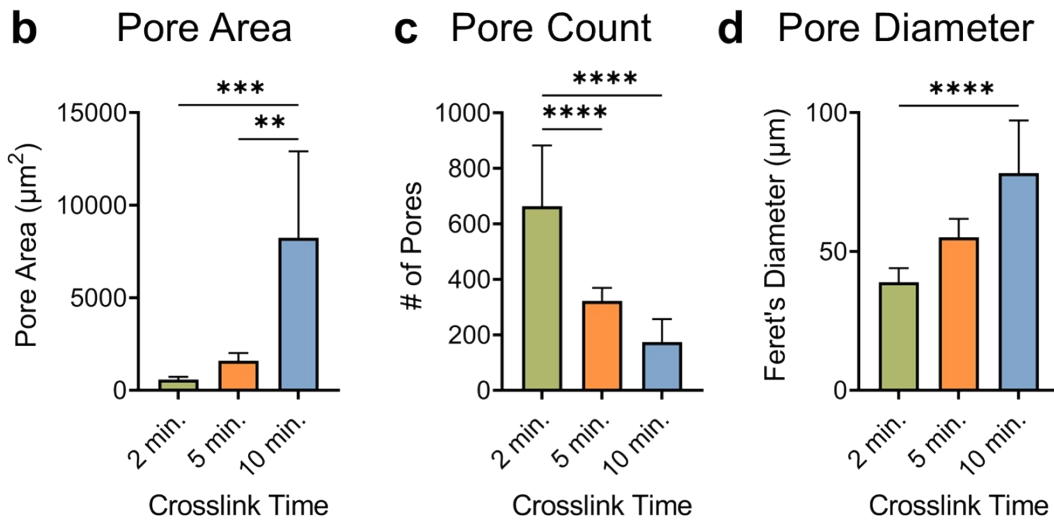
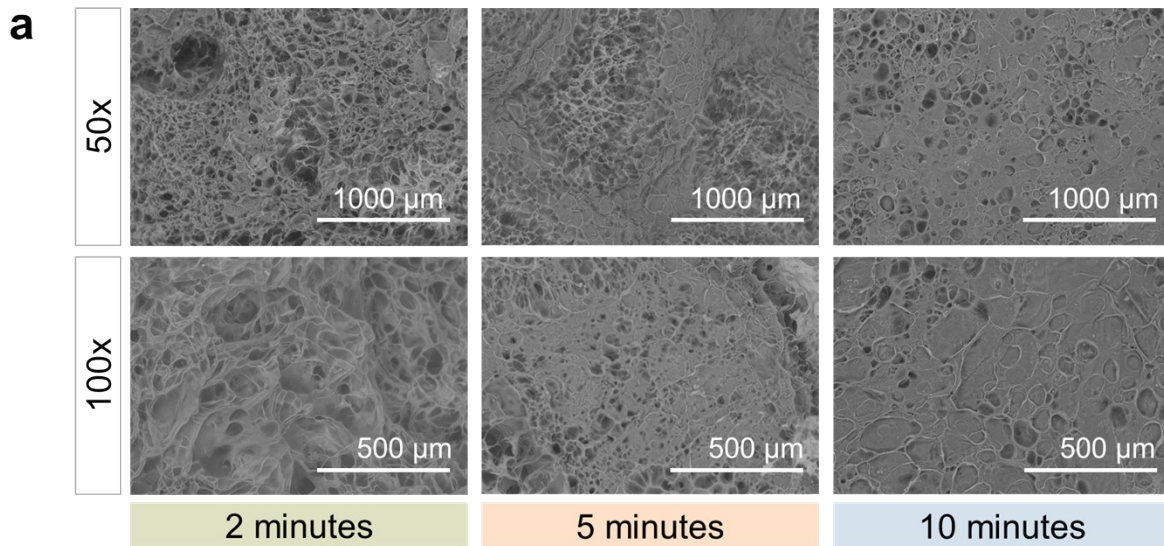


## Supplementary Information

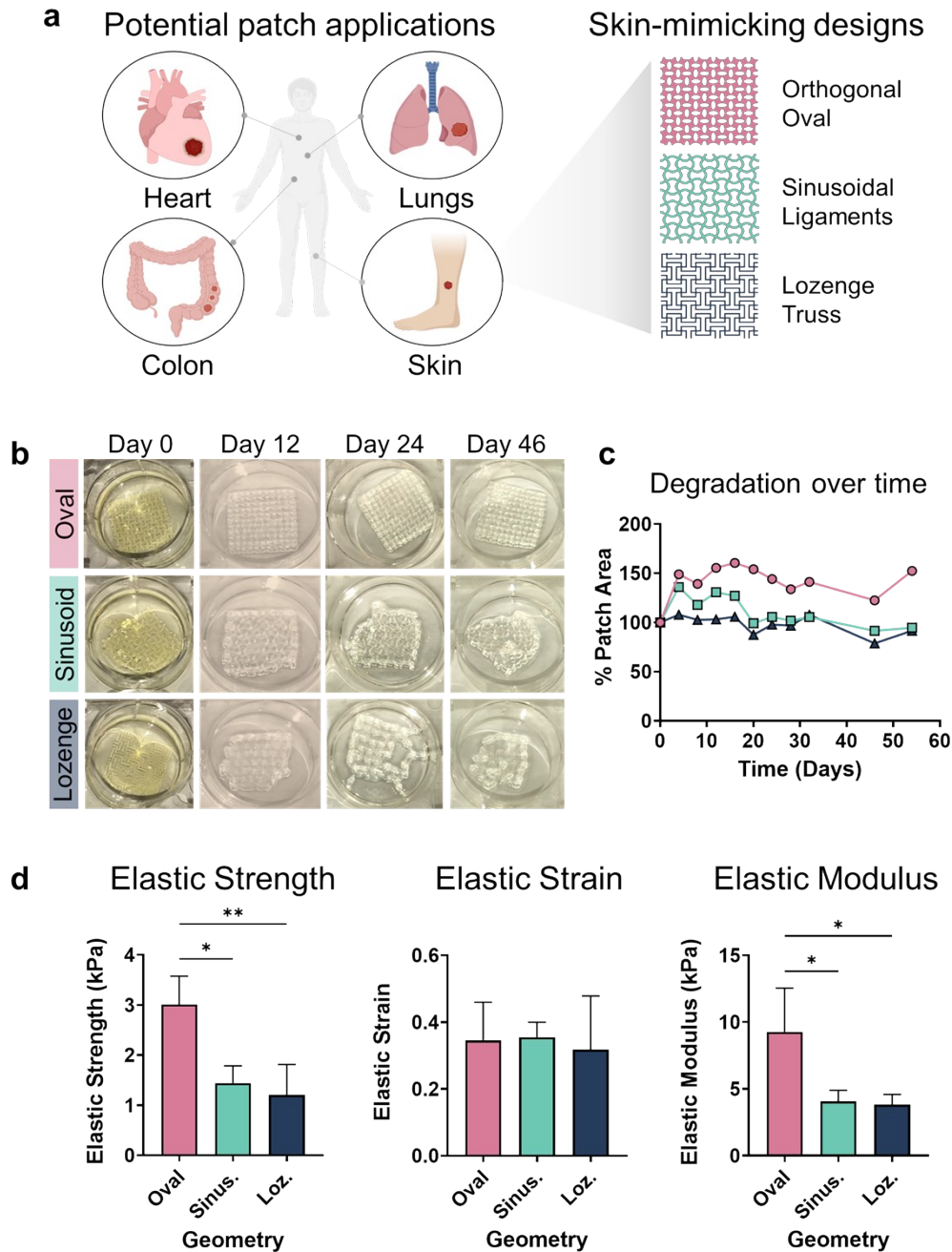
Emma L. Etter<sup>a,b</sup>, Mairead K. Heavey<sup>b</sup>, Matthew Errington<sup>b</sup>, and Juliane Nguyen<sup>a, b\*</sup>



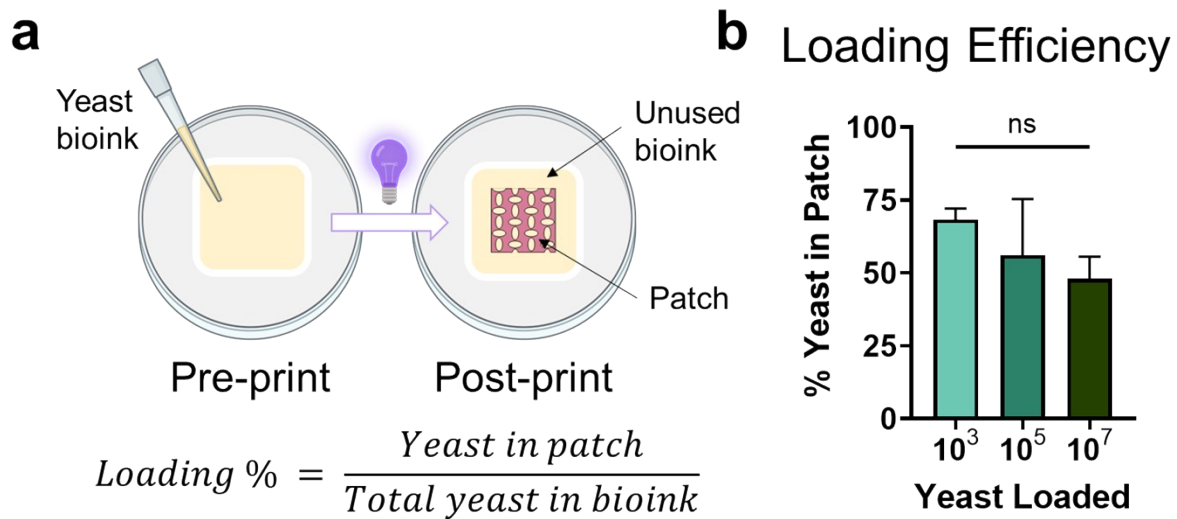
**Supplementary Figure 1. NMR spectra of gelatin versus 40% GeIMA.** Aromatic protons on the gelatin backbone are highlighted in green and were integrated before analysis. The reference D<sub>2</sub>O signal is highlighted in orange; (a) and (b) show methacrylamide group acrylic protons in lysines and hydroxylysines; (c) show protons in lysine groups on the gelatin backbone which were integrated to calculate degree of methacrylation (DOM); (d) show methyl protons of methacryloyl groups.



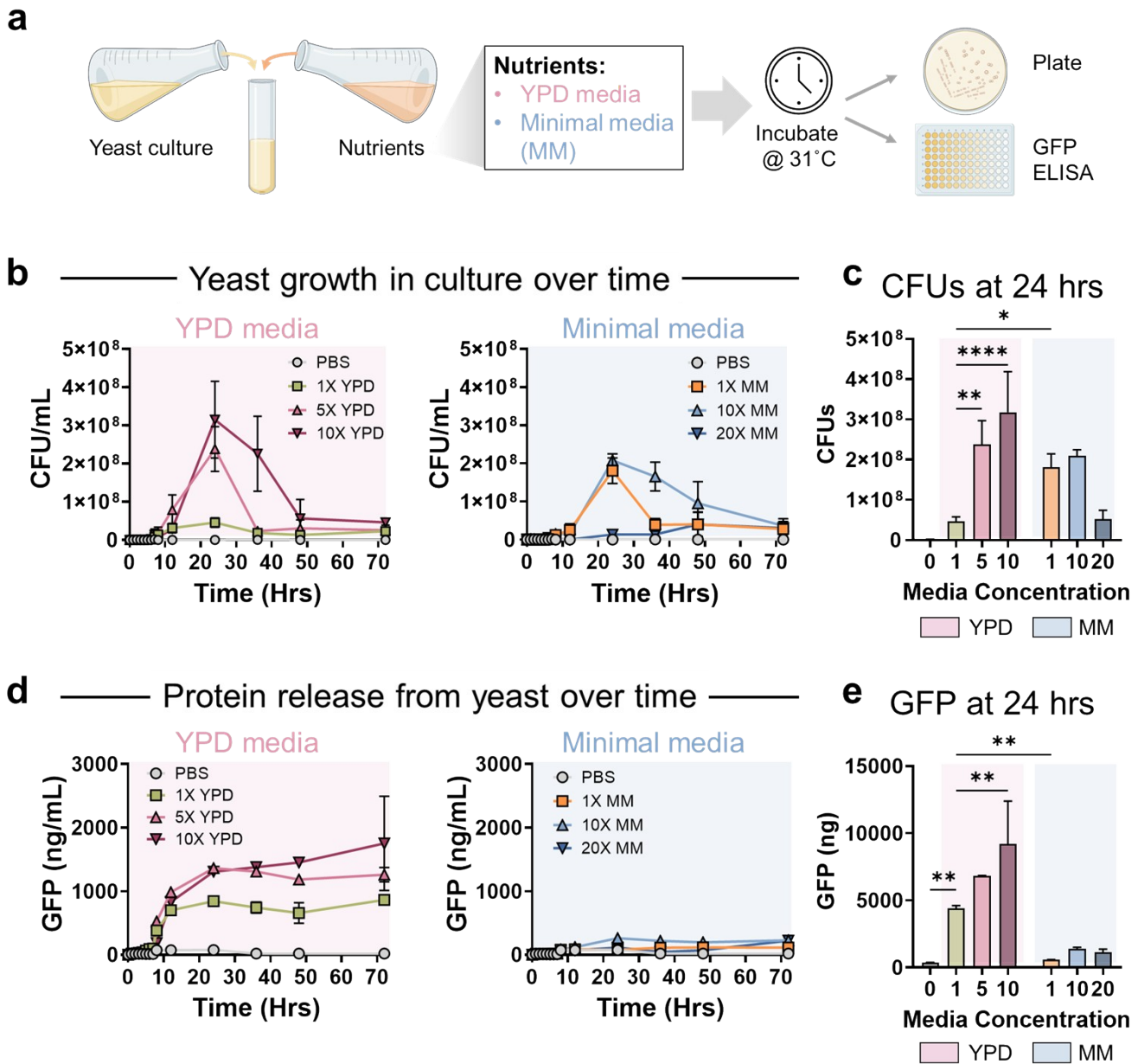
**Supplementary Figure 2. Patch pore size versus crosslink time. (A)** SEM images of patches with increasing crosslink time at two magnifications. **(B)** Average pore area calculated from these images. **(C)** The number of pores present in a consistent square of patches. **(D)** The average diameter of pores in these patches. Data are presented as mean  $\pm$  SD,  $n=3$ , with  $*p<0.05$ ,  $**p<0.01$ ,  $***p<0.001$ , and  $****p<0.0001$  by one-way ANOVA followed by Dunnett's multiple comparisons test using GraphPad Prism.



**Supplementary Figure 3. The degradation and tensile mechanical properties of skin-mimicking patch geometries as a function of pore size. (A)** Patch geometries used are the same as in Figure 1 (oval, sinusoidal ligament, and lozenge truss). These were chosen as examples of skin-mimicking geometries for potential wound healing applications. **(B)** Images of the patches at time points up to 46 days to show how patch geometry/integrity differs between these geometries over time. **(C)** Plot of patch area over time. **(D)** Elastic strength, strain, and modulus of these three geometries determined using tensile testing. Data are presented as mean  $\pm$  SD,  $n=3$ , with  $*p<0.05$ ,  $**p<0.01$ , by one-way ANOVA followed by Dunnett's multiple comparisons test using GraphPad Prism.



**Supplementary Figure 4. (A)** Schematic of yeast loading into patches and equation used for calculating loading efficiency. Increasing amounts of yeast cells were loaded into the bioinks. A sample was taken and plated before printing. After patch printing, a sample of the uncrosslinked bioink was taken to calculate the number of cells that were not encapsulated. **(B)** Loading efficiency as a function of yeast concentration. Data are presented as mean  $\pm$  SD,  $n=3$ , with  $*p<0.05$  by one-way ANOVA followed by Dunnett's multiple comparisons test using GraphPad Prism.



**Supplementary Figure 5. Yeast growth and GFP release in culture with different concentrations of growth media. (A)** Experimental workflow of how nutrients were added into yeast cultures and how their effects were tested. **(B)** Yeast growth over time (CFU/mL) with increasing concentrations of YPD and MM. **(C)** Yeast CFU/mL at 24 h to compare all groups. **(D)** GFP release with increasing concentrations of YPD and minimal medium. **(E)** GFP concentration in all media at 24-hour timepoint, representative of the maximum amount of GFP present during the measured timeframe. Data are presented as mean  $\pm$  SD,  $n=3$ , with  $*p<0.05$ ,  $**p<0.01$ ,  $***p<0.001$ , and  $****p<0.0001$  by one-way ANOVA followed by Dunnett's multiple comparisons test using GraphPad Prism.